OP rule] would have a much broader peak than that for the πN, KN, NN, and $N\bar{N}$ reactions. In fact, we can now predict

$$d\sigma(\eta p \to \eta p)/dt = \pi[\tilde{A}_{\eta p} \exp(\tfrac{1}{2}\gamma_{\eta p} t)]^2 = 30 \exp(3.6t) \text{ mb } (\text{BeV}/c)^{-2}. \quad (30)$$

Also, from Eq. (14),

$$\sigma^{\text{tot}}(\eta p) \simeq 21 \text{ mb}. \quad (31)$$

Unfortunately, these cross sections are not particularly easy to measure at high energies.

Finally, if two differential cross sections for reactions of the type $P+B \to P'+$hyperon (e.g., $\pi^- p \to K^+\Sigma^-$, $K^- p \to \pi^-\Sigma^+$, etc.) were measured, then a similar search would yield enough information to determine all five constants in Eq. (14), so that all PB total cross sections could be predicted.

The author wishes to thank Professor W. D. McGlinn, Professor S. K. Bose, and Professor P. C. DeCelles for numerous fruitful discussions and for reading the manuscript. He is also indebted to Dr. K. C. Wali for some useful comments. Finally, the parameter search would not have been possible without the generous assistance of Professor W. R. Johnson.

PHYSICAL REVIEW VOLUME 160, NUMBER 5 25 AUGUST 1967

Further Studies of a Recent Regge Representation

W. J. ABBE*
Physics Department, University of Michigan, Ann Arbor, Michigan

AND

G. A. GARY
Physics Department, University of Georgia, Athens, Georgia

(Received 7 April 1967)

The modified Cheng representation (MCR) is evaluated for S, P, and D waves with the potentials $-1.8e^{-r}/r$ and $-5e^{-r}/r$, the former being strong enough to have one bound state near the S-wave threshold, while the latter is nearly strong enough to have a P-wave resonance. We find good agreement with exact results with only one trajectory input, the agreement being better than the Cheng representation (CR) with three trajectories. Although both representations, the MCR and the CR, are automatically unitary, the results are a considerable imporvement over the earlier modified Khuri representation, which was not unitary—especially for the more attractive potential $-5e^{-r}/r$. Residues above threshold are also calculated and compared with the exact results, while reduced residues both above and below threshold are calculated via the MCR, and in all cases good agreement with exact results is obtained. Finally, a simple approximation to the reduced residue below threshold is noted to be quite accurate in potential theory, and may provide a simple and accurate means of estimating high-energy total cross sections and diffraction widths.

I. INTRODUCTION

THE remarkable success of quantum electrodynamics (QED) in understanding electromagnetic interactions has unfortunately not greatly aided in the calculation of strong-interaction cross sections, although physical analogies are often made. For example, in the same sense that one envisions the force between an electron and a proton in an hydrogen atom as being a consequence of the exchange of virtual photons, one may think of the force between a proton and a neutron in a deuteron as resulting from the exchange of π mesons. If one were to follow a strict analogy with QED, insofar as calculating strong-interaction energy levels is concerned, then one might approximate the force between two strongly interacting particles by a single virtual-pion exchange, in the same sense that Coulomb's law may be thought of as resulting from a single virtual photon exchange between two electrically charged particles. One would then insert this potential into a Schrödinger equation and calculate the bound states of the system. The relativistic corrections would then be calculated via the relativistically invariant Born series or Feynman technique as in QED.

However, three fundamental differences between the electromagnetic force problem and the nuclear force problem have precluded such a procedure:

(a) Since a single-particle exchange graph gives the force between two particles to order $g^2/\hbar c$ where g^2 is the coupling strength, the approximation is not a bad one for electromagnetic (EM) interactions, since this ratio is $\approx 1/137$; however, for strong interactions this ratio is

* Institute of Science & Technology Fellow on leave from the University of Georgia, Athens, Georgia.

≈ 1, so it is not clear that the first term is an adequate approximation to the potential.[1]

(b) In contrast to EM interactions, where only the photon can be exchanged, nuclear forces may arise via the exchange of many particles; for example, the π-N system can exchange π, ρ, f^0, N, $\cdots$ to name but a few. Thus the potential is, in general, orders of magnitude more complicated.

(c) It is not clear how to construct a relativistic generalization of the Schrödinger equation, which, although it gave a good approximation to the hydrogen energy levels because of the fairly low relative velocity between electron and proton ($v/c \approx 1/137$), cannot be used reliably for calculating energy levels when the relative velocity between particles is comparable to c, the velocity of light, as it often is in high-energy experiments.

In short, when one speaks of the "success of QED," one means in the calculation of corrections to the bound-state problem, assuming that the latter has already been solved approximately; it is just at the level of the bound-state problem where one has stumbled in the case of the hadrons or strongly interacting particles. The difficulties (a), (b), and (c) above do not include the various renormalization problems with particular Feynman graphs, which are still a subject for debate even for QED.

One feels intuitively that whatever form a complete theory of strong interactions may ultimately take, at least it should reduce to a Schrödinger equation with an appropriate potential in a nonrelativistic or "correspondence principle" limit. One may therefore attempt to construct a relativistic theory by essentially reversing the procedure; that is, one may construct a theory which possesses those properties that the Schrödinger theory possesses; for example, linear superposition of states, unitarity of the S matrix, correct threshold behavior of the phase shift, etc. This, then, provides the primary motivation for studying the solutions of the Schrödinger equation for classes of short-range potentials.

The connection with the relativistic problem is then made via the Møller rules for constructing a relativistically invariant scattering amplitude,[2] along with the crossing relations, or relations connecting particle and antiparticle amplitudes, which in turn have given rise to the bootstrap hypothesis.[3] One could have proceeded more directly by constructing relativistically invariant Lagrangian field theories in a first- or second-quantized form, the variation of which yields the relativistic "Schrödinger" equations which, in general, turn out to be complicated nonlinear differential equations for the probability amplitudes or field operators. However, the crossing relations, when written in terms of invariant amplitudes, lead to nonlinear equations of an integral form; the main advantage of the S-matrix theory as opposed to a Lagrangian theory appears to lie in the fact that the boundary conditions have already been imposed, as is usually the case with integral equations, whereas they must be imposed on the differential equations. Moreover, with the S-matrix theory, since one is working with directly measurable quantities, one can "cheat" and relatively easily compare (preliminary) results with experiment. However, both approaches lead to complicated nonlinear equations, differential or integral.

Recent attempts to construct a scattering amplitude represented in terms of angular-momentum poles have led to representations for the partial-wave amplitude[4] and total scattering amplitude[5] which compared quite well to exact results for a single Yukawa potential $-1.8e^{-r}/r$; the exact results were calculated from a direct integration of the Schrödinger equation performed by Ahmadzadeh.[6] The representation was then further studied by developing some π-N phenomenology[7] and an approximate bootstrap calculation of the ρ meson,[8] again yielding results in quite good agreement with experiment; for example, the latter calculation (Ref. 8) yielded a "best" width of the ρ of about 125 MeV, in contrast with other calculations which yield widths as large as 600 MeV,[9] while the experimental value is known to be about 106 MeV. Finally, in a recent calculation by Nath, Srivastava, and Vasavada, the equations were used to bootstrap the K^* (891-MeV)

[1] Not infrequently, one finds statements implying that since the quantity Gm^2/hc (where m is the mass involved in the self-interaction of the particle) for gravitational interactions is about 10^{-39}, therefore gravitation could not account for nuclear forces. [M. Gell-Mann and Y. Ne'eman, *The Eight-Fold Way* (W. A. Benjamin, Inc., New York, 1964), p. 1; R. P. Feynman, California Institute of Technology report (unpublished).] However, the gravitational problem is fundamentally different from the electromagnetic problem, the difference arising from the nonlinearity of the vacuum gravitational field equations, in contrast to the corresponding Maxwell equations which are linear. The truth of such statements that gravitation is necessarily a weak force is therefore not evident, especially when they are based on a perturbation expansion and not on a complete solution of the gravitational field equations. Indeed, Efinger [H. J. Efinger, Acta Phys. Austriaca **17**, 348 (1964); **19**, 264 (1965)] has shown, by solving the full nonlinear gravitational field equations *exactly*, that one can construct a stable charged particle wherein gravitational attraction balances electrical repulsion; as he has stressed, however, if a perturbation expansion in powers of G has been made, no solution would have obtained [H. J. Efinger (private communication); Nuovo Cimento (to be published)]. Other authors have also obtained a self-consistent solution, although from a somewhat different point of view. [R. Arnowitt, S. Deser, and C. W. Misner, *Gravitation, An Introduction to Current Research* (John Wiley & Sons, Inc., New York, 1962), Chap. 5, p. 227. Relevant references are given here.]

[2] C. Møller, Kgl. Danske Videnskab. Selskab, Mat.-Fys. Medd. **22**, No. 19 (1946); **23**, No. 1 (1945).

[3] G. F. Chew and S. C. Frautschi, Phys. Rev. Letters **7**, 394 (1961).

[4] W. J. Abbe, P. Kaus, P. Nath, and Y. N. Srivastava, Phys. Rev. **140**, B1595 (1965).

[5] W. J. Abbe, P. Kaus, P. Nath, and Y. N. Srivastava, Phys. Rev. **141**, 1513 (1966).

[6] A. Ahmadzadeh, Phys. Rev. **133**, B1074 (1964); A. Ahmadzadeh, P. G. Burke, and C. Tate, *ibid.* **131**, 1315 (1963); A. Ahmadzadeh, Ph.D. thesis, University of California Radiation Laboratory Report No. UCRL-11096, 1963 (unpublished).

[7] W. J. Abbe, P. Nath, and Y. N. Srivastava, Nuovo Cimento **45**, 675 (1966).

[8] W. J. Abbe, P. Kaus, P. Nath, and Y. N. Srivastava, Phys. Rev. **154**, 1515 (1967).

[9] M. Bander and G. Shaw, Phys. Rev. **135**, B267 (1964).

resonance of the π-K system, with even better satisfaction of the crossing relations than in Ref. 8.[10]

The purpose of this paper is to study the representation further by exhaustively comparing it with the exact results for a more attractive, and indeed the only other, potential for which extensive exact results are available at the present time: $-5e^{-r}/r$. This potential is almost strong enough to produce a P-wave resonance. The relevant equations are discussed in the next section, while results and graphs are discussed in Sec. III. Again, we will find favorable agreement between the partial-wave amplitudes, residues, and reduced residues. This evidence, coupled with that outlined above, may therefore make one a little less hesitant about using the representation for relativistic calculations of scattering amplitudes and cross sections.

II. DISCUSSION OF EQUATIONS

The Cheng representation (CR) for the single, elastic, two-body S-matrix element $S(l,s)$, written in terms of angular momentum poles $\alpha_n(s)$, has the form[11]

$$S(l,s)=\exp\left\{\sum_{n=1}^{\infty}\int_{\alpha_n(s)}^{\alpha_n^*(s)}\frac{e^{(l'-l)\xi}}{l'-l}dl'\right\}\equiv\exp\{2i\delta_l(s)\}, \quad (1)$$

where $\cosh\xi=1+\mu^2/2s$ with μ the lowest mass >0 in the potential distribution, s is the nonrelativistic energy, l is the usual angular momentum, and $\delta_l(s)$ is the usual phase shift. The CR has several important properties required of an S matrix, namely:

(i) $S(l,s)S^*(l^*,s)=1$, independent of the number of terms in the sum (1).

(ii) The phase shift $\delta_l(s)\to_{s\to 0} s^{l+1/2}$ has the correct threshold behavior, also independent of the number of terms of the sum (1).

The partial-wave amplitude $f_l(s)$ is defined as

$$f_l(s)=(S(l,s)-1)/2i\sqrt{s}, \quad (2)$$

and if we define $\beta_n(s)$ to be the residue of $f_l(s)$ at the pole $l=\alpha_n(s)$, we have for the CR

$$s^{l/2}\beta_n(s)=\mathrm{Im}\alpha_n(s)\exp\left\{\int_{\alpha_n}^{\alpha_n^*}\frac{e^{(l'-\alpha_n)\xi}-1}{l'-\alpha_n}dl'\right\}\times\exp\left\{\sum_{m\neq n}\int_{\alpha_m}^{\alpha_m^*}\frac{e^{(l'-\alpha_n)\xi}}{l'-\alpha_n}dl'\right\}. \quad (3)$$

The reduced residue $b_n(s)$, which is real-analytic in the s plane with only a right-hand cut for $s>0$, is defined as[12]

$$b_n(s)=\beta_n(s)/s^{\alpha_n(s)}. \quad (4)$$

[10] P. Nath, Y. N. Srivastava, and K. Vasavada (to be published); Bull. Am. Phys. Soc. 12, 472 (1967).

[11] H. Cheng, Phys. Rev. 144, 1237 (1966).

[12] J. R. Taylor, Phys. Rev. 127, 2257 (1962).

In a previous report,[4] the CR was studied in a one-trajectory approximation [one term of the sum (1)], and compared with exact results for the potential $-1.8e^{-r}/r$; this potential is strong enough to produce one bound state just below threshold. An attempt to improve the comparison with the exact S matrix for S waves as well as for the residue was the primary motivation for the modified-Cheng representation (MCR), in which the Born term for the phase shift is explicitly exhibited. The MCR of the S matrix, which has been derived in Ref. 4 and discovered independently by Blue,[13] may be written for a single Yukawa potential $-g^2e^{-\mu r}/r$:

$$S(l,s)=\exp\{(ig^2/\sqrt{s})Q_l(\cosh\xi)\}\prod_{n=1}^{\infty}S_n(l,s), \quad (5)$$

where

$$S_n(l,s)=\exp\left\{\int_{\alpha_n}^{\alpha_n^*}\frac{\exp[(l'-l)\xi]}{l'-l}dl'-\frac{ig^2}{\sqrt{s}}\frac{\exp[-(l+n)\xi]}{l+n}P_{n-1}(\cosh\xi)\right\}, \quad (6)$$

and the symbols are as defined above except that $\cosh\xi=1+(2\mu)^2/2s$, and $P_\nu(z)$ and $Q_\nu(z)$ are, respectively, Legendre functions of the first and second kinds. The generalization of (5) for a general superposition of Yukawa potentials, as well as one possible extension to relativistic processes, has been given.[5,14] Again, as in (3) above, the residue of the partial-wave amplitude may be identified for the MCR to be

$$s^{1/2}\beta_n(s)=\mathrm{Im}\alpha_n(s)\exp\left\{\int_{\alpha_n}^{\alpha_n^*}\frac{\exp[(l'-\alpha_n)\xi]-1}{l'-\alpha_n}dl'-\frac{ig^2}{\sqrt{s}}\frac{\exp[-(\alpha_n+n)\xi]}{\alpha_n+n}P_{n-1}(\cosh\xi)\right\}\times\exp\{(ig^2/\sqrt{s})Q_{\alpha_n}(\cosh\xi)\}\prod_{m\neq n}S_m(\alpha_n,s), \quad (7)$$

the reduced residue being defined in (4), with the residue now given by (7).

The MCR shares the important properties (i) and (ii) above with the CR; however, at large energies it also goes to its correct Born term, and there was a great improvement in the subsequent comparison of the S

[13] J. Blue, Ph.D. thesis, California Institute of Technology, 1966 (unpublished). Here the MCR was applied to an approximate bootstrap calculation of the ρ meson, using a scheme of coupled integral equations for trajectory parameters given previously [S. C. Frautschi, P. E. Kaus, and F. Zachariasen, Phys. Rev. 133, B1607 (1964)] and studied also by Hankins, Kaus, and Pearson. [D. Hankins, P. Kaus, and C. J. Pearson, *ibid.* 137, B1034 (1965); D. Hankins, Ph.D. thesis, University of California, Riverside, California, 1965 (unpublished); C. J. Pearson, Ph.D. thesis, University of California, Riverside, California, 1965 (unpublished).]

[14] W. J. Abbe, Ph.D. thesis, University of California, Riverside, California, 1966 (unpublished).

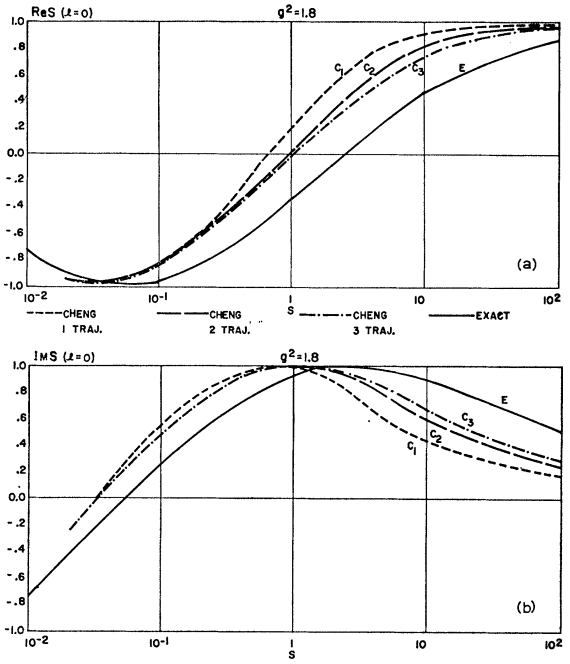

FIG. 1. (a) The real part and (b) the imaginary part of $S(0,s)$ for the CR with 1, 2, and 3 trajectories, compared with the exact result (E), for the potential $-1.8e^{-r}/r$, is plotted versus the energy s.

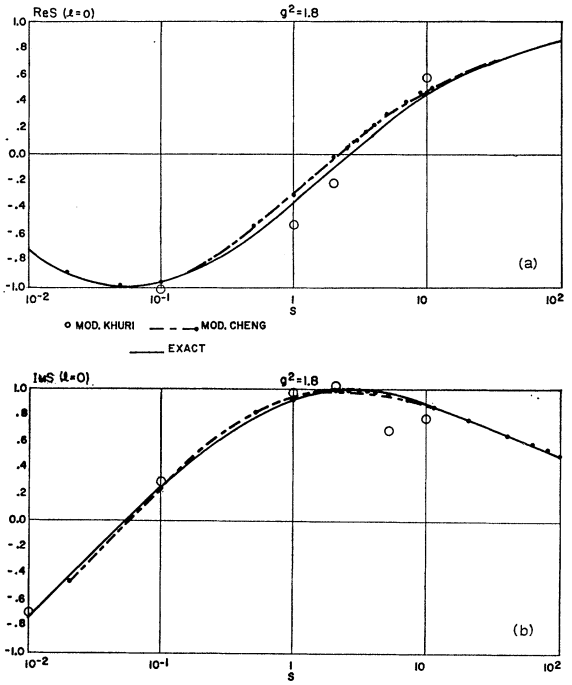

FIG. 2. (a) The real part and (b) the imaginary part of $S(0,s)$ for the MCR and MKR is compared with the exact result for the potential $-1.8e^{-r}/r$.

matrix [Eq. (5)] for S waves, and of the residue [Eq. (7)] for the potential $-1.8e^{-r}/r$, again in a one-trajectory approximation.[4] The purpose of this paper is to exhaustively compare the MCR for the S matrix and its corresponding residue, both in a one-trajectory approximation, with exact results for the stronger potential $-5e^{-r}/r$, which is, as noted above, the only

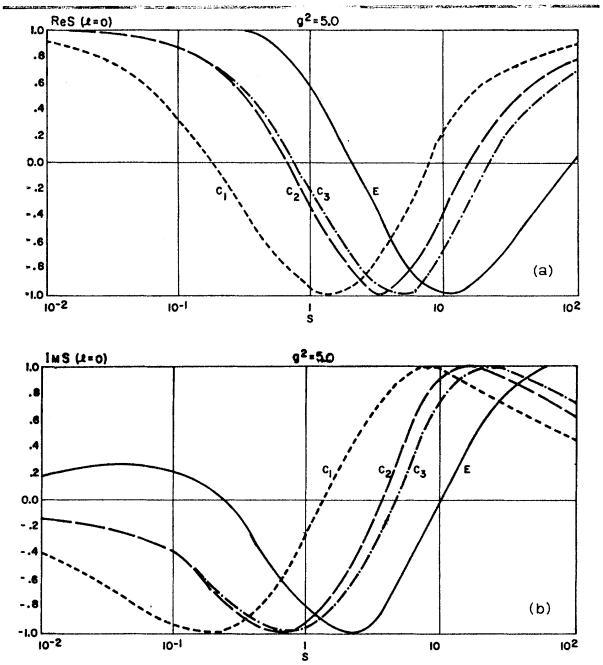

FIG. 3. The same as Fig. 1 except that the potential is $-5e^{-r}/r$.

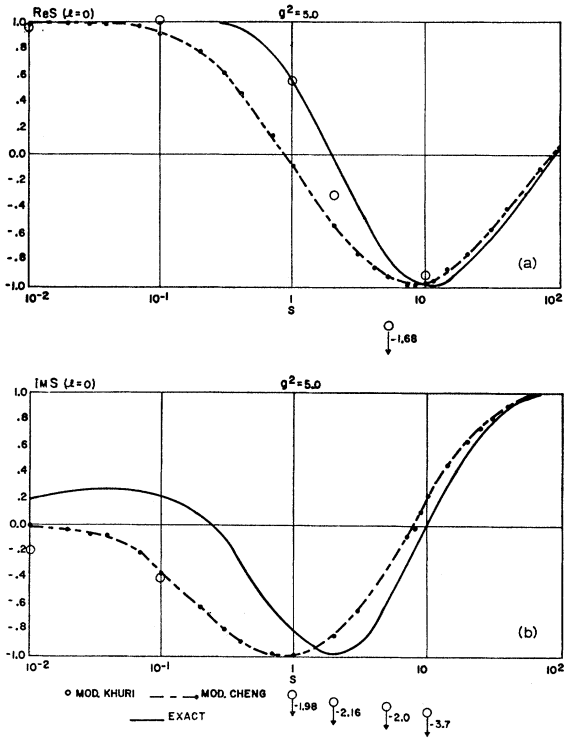

FIG. 4. The same as Fig. 2 except that the potential is $-5e^{-r}/r$.

other potential for which extensive exact results are at the present time available.[6] The relativistic calculation of scattering amplitudes via angular-momentum poles requires the reduced residue $b_n(s)$ for $s<0$, so we also

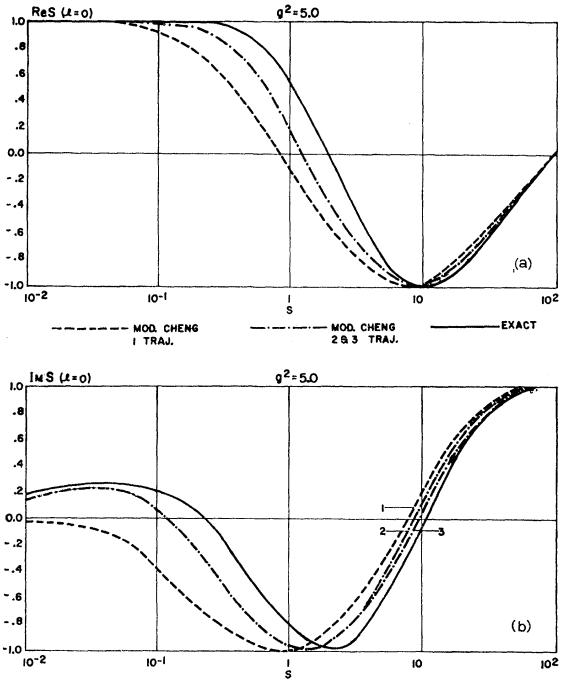

FIG. 5. (a) The real part and (b) the imaginary part of $S(0,s)$ for the MCR evaluated with 1, 2, and 3 trajectories is compared with the exact result.

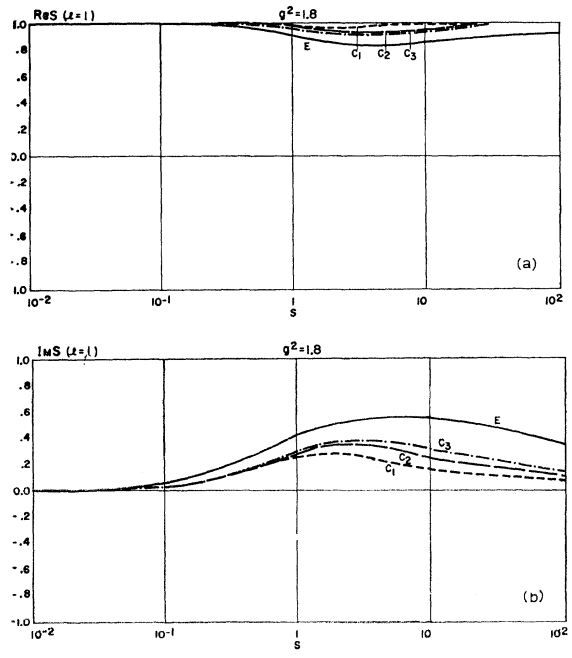

FIG. 6. (a) The real part and (b) the imaginary part of $S(1,s)$ is plotted versus the energy s as in Fig. 1.

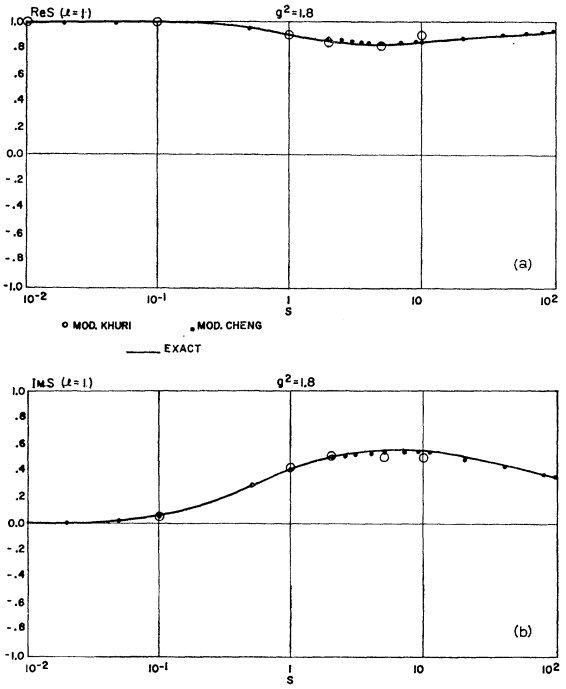

FIG. 7. (a) The real part and (b) the imaginary part of $S(1,s)$ for the MCR and MKR as in Fig. 2.

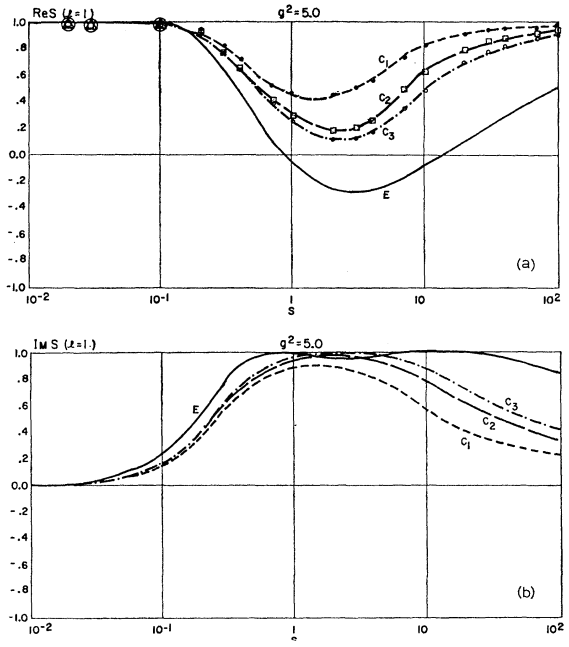

FIG. 8. (a) The real part and (b) the imaginary part of $S(1,s)$ is plotted for the CR with 1, 2, and 3 trajectories and the potential $-5e^{-r}/r$.

calculate this in a one-trajectory approximation and compare with the exact results. Since the derivation of the S matrix $S(l,s)$, and hence of $b_n(s)$, was made only for $s>0$ [as the unitarity condition (i) is, strictly speaking, valid only above threshold], we make the

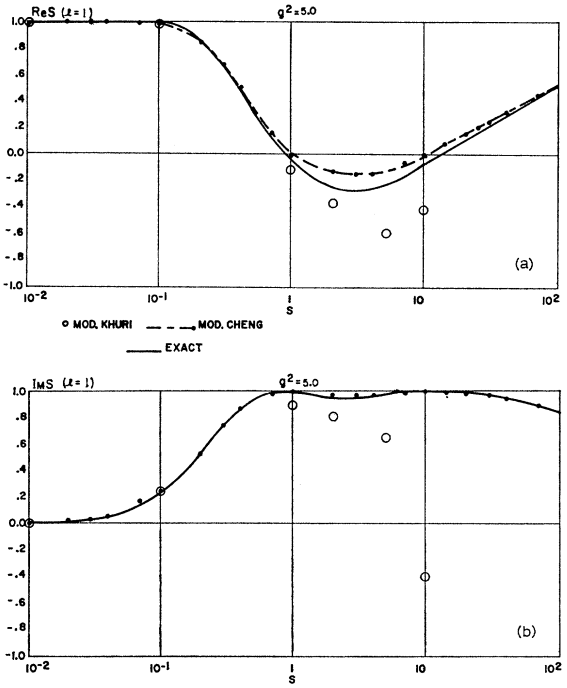

FIG. 9. (a) The real part and (b) the imaginary part of $S(1,s)$ for the MCR and MKR is plotted versus the energy s and compared with the exact result for the potential $-5e^{-r}/r$.

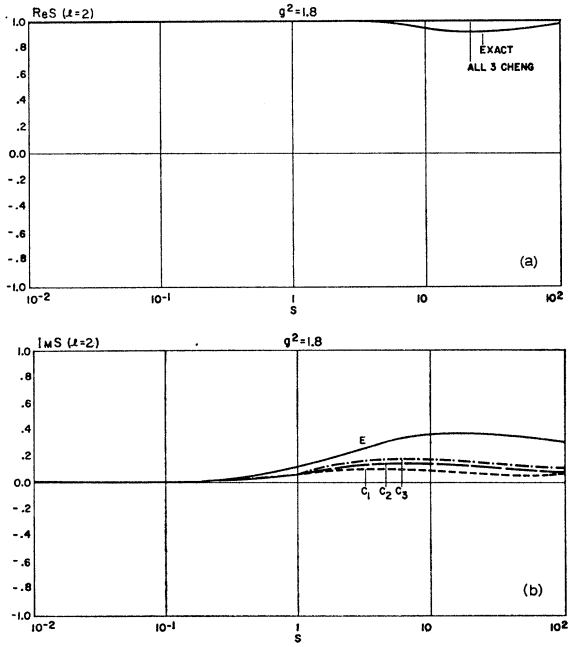

FIG. 10. (a) The real part and (b) the imaginary part of $S(2,s)$ for the CR with 1, 2, and 3 trajectories is plotted versus the energy s for the potential $-1.8e^{-r}/r$ and compared with the exact result.

continuation to $s<0$ via Cauchy's theorem:

$$b_n(s)=b_n(\infty)+\frac{1}{\pi}\int_0^\infty \frac{\mathrm{Im}b_n(s')}{s'-s-i\epsilon}ds', \quad \epsilon>0, \qquad (8)$$

where we have subtracted at $s=\infty$. It is not difficult to show that the integral (8) converges for the MCR given above without subtractions.

In the next section we compare the MCR with the

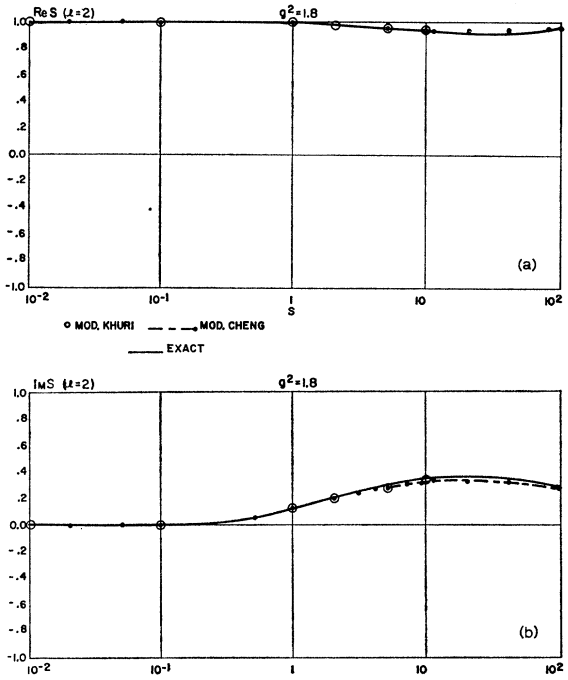

FIG. 11. (a) The real part and (b) the imaginary part of $S(2,s)$ for the MCR and MKR is plotted versus the energy s and compared with the exact result for the potential $-1.8e^{-r}/r$.

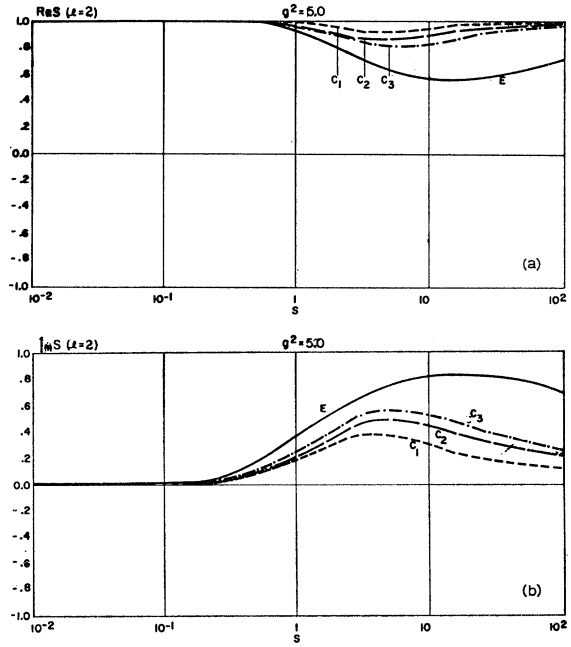

FIG. 12. (a) The real part and (b) the imaginary part of $S(2,s)$ is plotted for the CR with 1, 2, and 3 trajectories and compared with the exact result for the potential $-5e^{-r}/r$.

exact results, not only for the S matrix in a one-trajectory approximation for S, P, and D waves, but also for the residue and the reduced residue above threshold ($s>0$) and for the reduced residue when $s<0$.

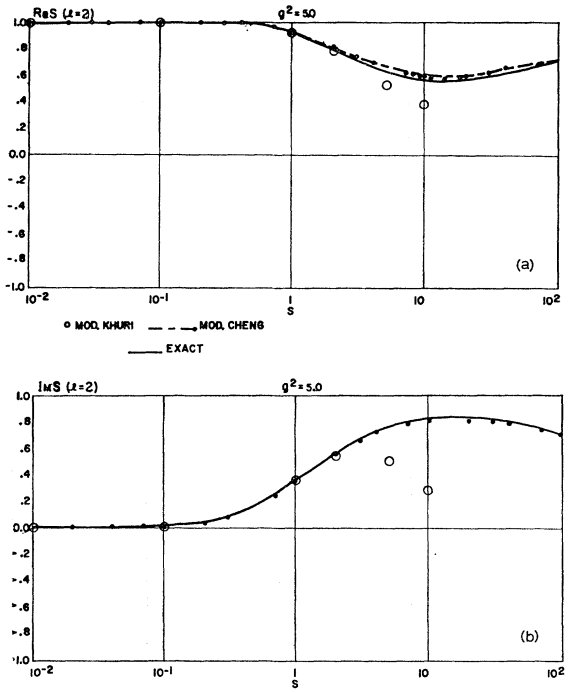

FIG. 13. (a) The real part and (b) the imaginary part of $S(2,s)$ is plotted for the MCR and MKR for the potential $-5e^{-r}/r$ and compared with the exact result.

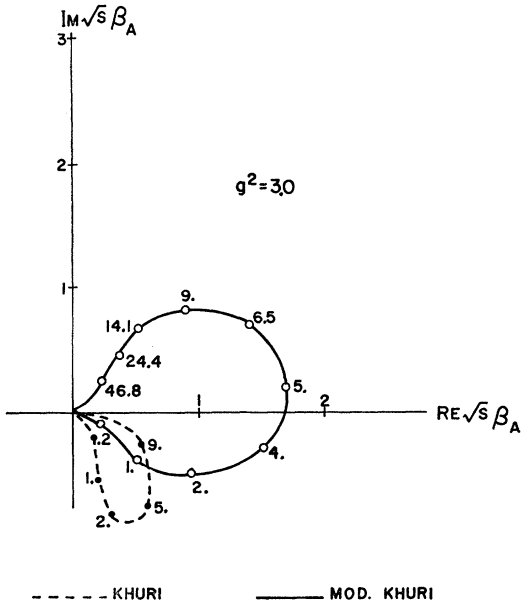

FIG. 14. The imaginary part of $s^{1/2}\beta(s)$ is plotted versus the real part of $s^{1/2}\beta(s)$ for both the Khuri representation and MKR as discussed in the text, with one trajectory input and the energy s given as a running parameter along the curves. The potential is $-3e^{-r}/r$.

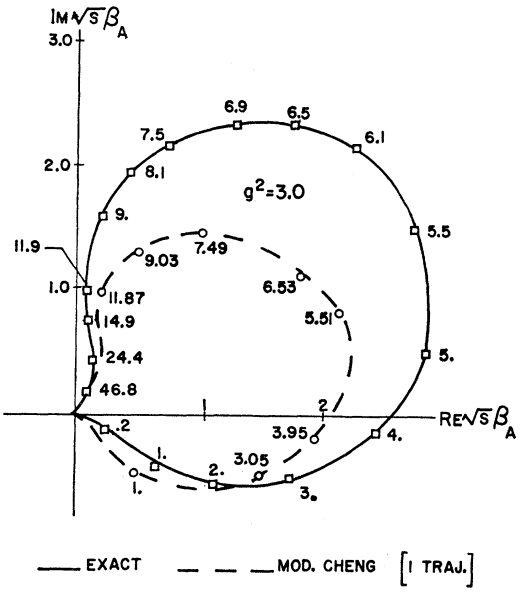

FIG. 15. The same as Fig. 14, except that now the MCR residue is evaluated with one trajectory and compared with the exact value.

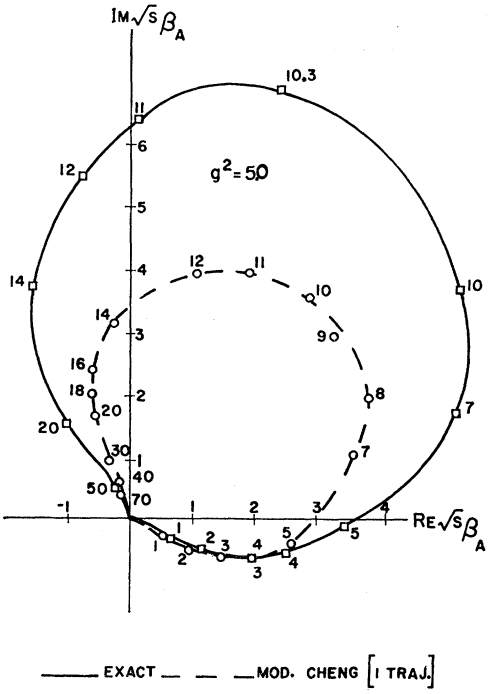

FIG. 16. The same as Fig. 15 except that the potential is $-5e^{-r}/r$.

Good agreement with the exact results is obtained for the potential $-5e^{-r}/r$, and it will be seen that one trajectory of the MCR is better than three trajectories of the CR. The purpose of making this last comparison is that since the CR is considerably simpler than the MCR, one is tempted to take more poles of the CR in lieu of one pole of the mathematically more complicated

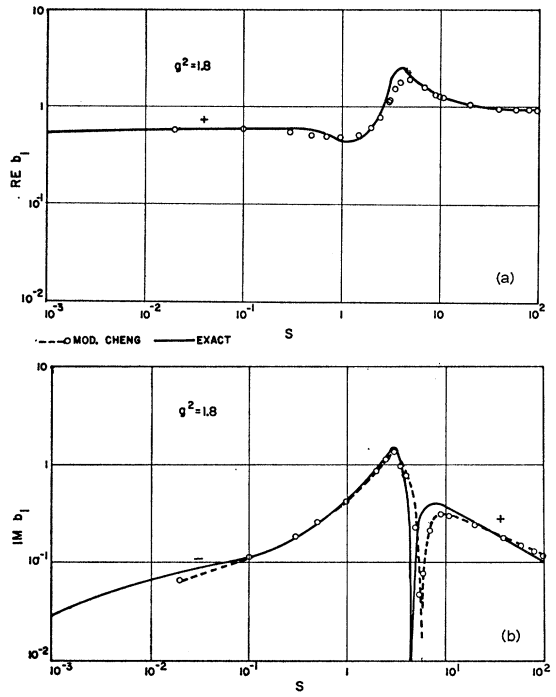

FIG. 17. (a) The real part and (b) the imaginary part of the reduced residue $b(s)$ is plotted for $s>0$ for the MCR with one trajectory and compared with the exact result for the potential of $-1.8e^{-r}/r$.

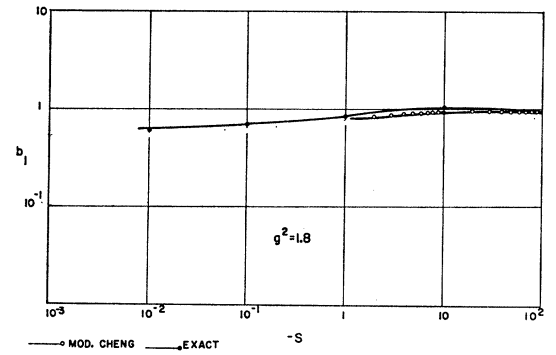

FIG. 18. The reduced residue $b(s)$ is plotted for s below threshold for the MCR with one trajectory for the potential $-1.8e^{-r}/r$ and compared with the exact result.

MCR. However, we shall see that even three poles of the CR cannot give an improvement over one pole of the MCR.[15] Finally, we also compare the S matrix for S, P, and D waves as calculated from the MCR with the earlier modified-Khuri representation (MKR) (Ref. 6 and S. C. Frautschi *et al.* cited in Ref. 13) for both potentials $-1.8e^{-r}/r$ and $-5e^{-r}/r$, and we shall see that the MCR is quite an improvement over the one-trajectory MKR.[16]

[15] Preliminary results of this work have been reported: W. J. Abbe and G. A. Gary, Bull. Am. Phys. Soc. 11, 901 (1966).

[16] It has been noted in Ref. 6 that as the potential strength increases, the residues become more difficult to calculate, and this could account for the rather erratic results reported there for the one-trajectory MKR when the potential is $-5e^{-r}/r$.

III. RESULTS

The results are presented in Figs. 1–21; most of the figures are self-explanatory. For example, all curves labeled E are from the exact integration of the Schrödinger equation.[6] The curves labeled C_1, C_2, and C_3 are the CR from Eqs. (1) and (3), evaluated with 1, 2, and 3 trajectories, respectively, the exact trajectories being used. The graphs are all labeled with the corresponding coupling constant, either 1.8 or 5, with several residue plots being given for a coupling constant of 3.

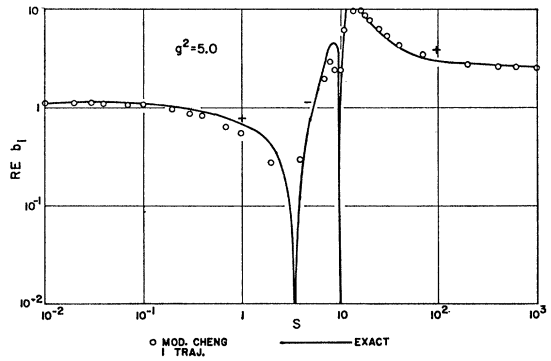

FIG. 19. The same as Fig. 17(b) except that now the potential is $-5e^{-r}/r$.

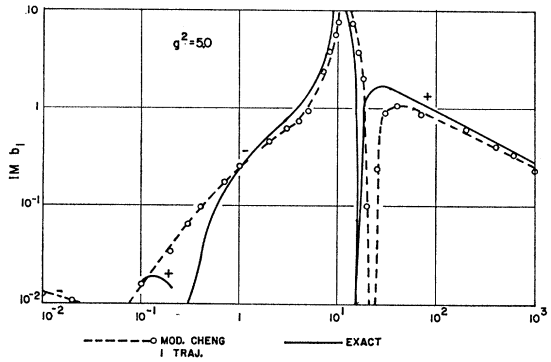

FIG. 20. The same as Fig. 18 for the imaginary part of $b(s)$ except that now the potential is $-5e^{-r}/r$.

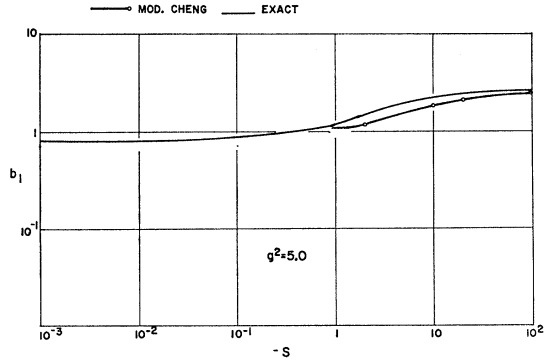

FIG. 21. The same as Fig. 18 for s below threshold except that now the potential is $-5e^{-r}/r$.

The first 13 figures give results for the S matrix for S, P, and D waves. The real or imaginary part of the S matrix is plotted versus the energy s, the latter being plotted on a logarithmic scale. For example, in Fig. 1 the real and imaginary parts of the CR, for the potential $-1.8e^{-r}/r$ and Eq. (1) above, are evaluated with 1, 2, and 3 trajectories and compared with the exact results; while in Fig. 2 the MCR is evaluated with *one* trajectory and compared with the exact results, as well as with the MKR (which is plotted as circles). Figures 1 and 2 are for S waves. Figures 3 and 4 show similar results for the stronger potential $-5e^{-r}/r$, again for S waves, while in Fig. 5 the convergence of the MCR is illustrated for S waves by evaluating it with 2 and 3 trajectories. Figures 6–9 give corresponding results for P waves, while the results for D waves are presented in Figs. 10–13. Except where otherwise noted, the MCR is always evaluated with *one* trajectory.

Since some exact residues have been calculated for the potential $-3e^{-r}/r$, Fig. 14 contains a plot of what corresponds to Eq. (3) for the quantity $s^{1/2}\beta(s)$, for both the Khuri and modified-Khuri representations (D. Hankins *et al.* cited in Ref. 13), so that a comparison with the MCR and the exact results in Fig. 15 can be made. In both of these graphs, $\mathrm{Re}s^{1/2}\beta(s)$ is plotted versus $\mathrm{Im}s^{1/2}\beta(s)$ with the energy s as a running parameter, one trajectory again being used. Similar results are given in Fig. 16 for the stronger potential $-5e^{-r}/r$, where the MCR with one trajectory is compared with the exact residue.

In Fig. 17 the real and imaginary parts of the reduced residue, defined in Eq. (4), are calculated above threshold via the MCR in a one-trajectory approximation and compared with the exact values for the potential $-1.8e^{-r}/r$. Figure 18 shows the results of evaluating the dispersion integral of Eq. (8) for $s<0$, again with the MCR in a one-trajectory approximation. Figures 19–21 show the corresponding results for the stronger potential $-5e^{-r}/r$.

The graphs speak pretty much for themselves, and we conclude that the MCR, in a one-trajectory approximation, gives quite good results even when the potential is almost strong enough to produce a P-wave resonance, as $-5e^{-r}/r$ is; the S matrix for the latter potential is greatly improved over the earlier MKR. Finally, the reduced residue $b(s)$ agrees very well with the exact value, both when the energy s is above threshold and when it is below. This is important for relativistic calculations in order that the high-energy cross sections and diffraction widths be predicted accurately.

We shall conclude by pointing out what may be a useful approximation. In a one-trajectory approximation, the reduced residue of both the CR and the MCR has the threshold behavior [from Eqs. (3), (4), and (7)]

$$b_1(s) \underset{s\to 0}{\longrightarrow} \frac{\mathrm{Im}\alpha_1(s)}{s^{\alpha_1(s)+1/2}}. \tag{9}$$

Now the threshold behavior of a trajectory with $\alpha_1(0)>-\frac{1}{2}$ is known to be[17]

$$\mathrm{Im}\alpha_1(s) \underset{s\to 0}{\longrightarrow} C_1 s^{\alpha_1(0)+1/2}, \tag{10}$$

where $\alpha_1(0)$ is the real part of $\alpha_1(s)$ evaluated at $s=0$. Therefore, to lowest order

$$b_1(s) \underset{s\to 0}{\longrightarrow} C_1, \tag{11}$$

and the reduced residue at threshold is essentially the "slope" of Imα above threshold. In a one-trajectory approximation, the slope may be roughly estimated to be ≈ 0.58 for the potential $-1.8e^{-r}/r$ and ≈ 1.03 for $-5e^{-r}/r$, to be compared with the exact reduced residues at threshold of ≈ 0.60 and ≈ 0.80, respectively. Since the graphs are difficult to read,[6] accurate values are difficult to calculate. However, we see that the simple one-trajectory reduced residue (11) provides quite a good approximation to the exact value at $s=0$, and indeed down to a substantial distance below threshold ($s<0$), since the exact $b_1(s)$ are nearly constant for $s<0$. This may provide a simple and yet fairly accurate method of calculating total high-energy cross sections and diffraction widths, which require $b(s)$ for $s<0$.[18]

We therefore conclude that the modified-Cheng representation, having been tested in a variety of situations[4,5,7,8,10,13] as well as in the present report, may provide a "believable" method for calculating relativistic two-body elastic amplitudes.[19]

---

[17] B. R. Desai and R. G. Newton, Phys. Rev. **130**, 2109 (1963).

[18] G. F. Chew and V. L. Teplitz, Phys. Rev. **136**, B1154 (1964).

[19] The extension of the MCR to inelastic processes has been carried out, although unfortunately there are not yet any exact results to compare with. W. J. Abbe, P. Nath, and Y. N. Srivastava, Nuovo Cimento (to be published).